

Supporting Information

High Temperature Ferromagnetic metal: Janus CrSSe monolayer

Yaxuan Wu,^{a,#} Qingquan Liu^{b,#} Puyuan Shi,^a Jingjuan Su,^a Yungeng Zhang,^{a} and
Bing Wang^{a*}*

^aJoint Center for Theoretical Physics (JCTP), Institute for Computational Materials Science, School of Physics and Electronics, Henan University, Kaifeng 475004, People's Republic of China.

^bPatent Examination Cooperation (Henan) Center of the Patent Office, China National Intellectual Property Administration, Zhengzhou 450000, People's Republic of China

#These authors have contributed equally to this work

* **E-mail:** 20130016@vip.henu.edu.cn; wb@henu.edu.cn

1. The POSCAR of CrSSe monolayer.

CrSSe

```
1.0000000000000000
 3.3893135380526203  0.0000000000000000  0.0000000000000000
-1.6946567690263101  2.9352309615695544  0.0000000000000000
 0.0000000000000000  0.0000000000000000  20.4300003052000001
Cr S Se
 1  1  1
```

Direct

```
0.6666666972774706  0.3333333537098753  0.4955543581952639
0.3333331930868226  0.6666668599245682  0.4317737194445215
0.0000001676357044  0.9999998323655603  0.5793419473602057
```

2. Poisson's ratio and Young's modulus of CrSSe monolayer

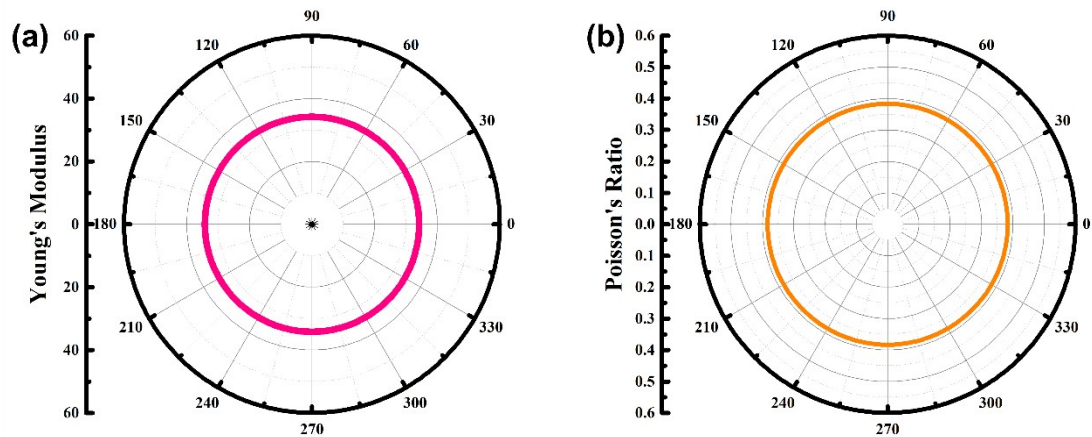


Figure S1 Calculated orientation-dependent Poisson's ratio (a), and Young's modulus (b).

3. The phase diagrams of CrSSe monolayer

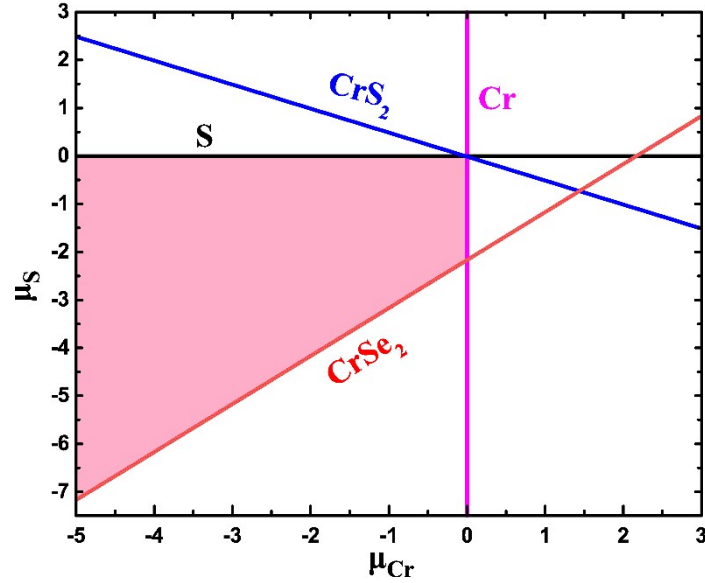


Figure S2 The phase diagrams of CrSSe monolayer.

Target compound can be synthesized by careful control of chemical potential during experimental synthesis. The chemical potentials of constituent species can be varied to reflect specific equilibrium growth conditions, and they are globally constrained by the formation enthalpy of the host to maintain its stability. In order to better explain the dynamic stability of CrSSe monolayer, we also introduce the chemical potential to draw the thermodynamic stability diagram¹⁻⁴. we define the formation enthalpy (ΔH) of CrSSe monolayer at 0 K as:

$$\Delta H = \frac{E_{CrSSe} - \mu_{Cr} - \mu_S - \mu_{Se}}{3} \quad (1)$$

where E_{CrSSe} are the energy of CrSSe monolayer; μ_{Cr} , μ_S , μ_{Se} are the chemical potential of Cr, S, and Se atom in their most stable solid phase.

The formation enthalpy in CrSSe monolayer needs to satisfy:

$$\mu_{Cr} + \mu_S + \mu_{Se} = \Delta H_f^{CrSSe}$$

Besides, the chemical formula in the CrSSe monolayer must also be restricted to other possible competing phases, for example,

$$\mu_{Cr} + 2\mu_{Se} \leq \Delta H_f^{CrSe_2}$$

$$\mu_{Cr} + 2\mu_S \leq \Delta H_f^{CrS_2}$$

For our studied compound (CrSSe monolayer), we calculate the accessible range of chemical potential (pink shaded region) for the equilibrium growth conditions of CrSSe monolayer as shown in Figure S2 at the Supplemental Material. From the calculated accessible range of chemical potential, CrSSe monolayer can be synthesized under equilibrium growth conditions.

4. The FM state and AFM states of CrSSe monolayer.

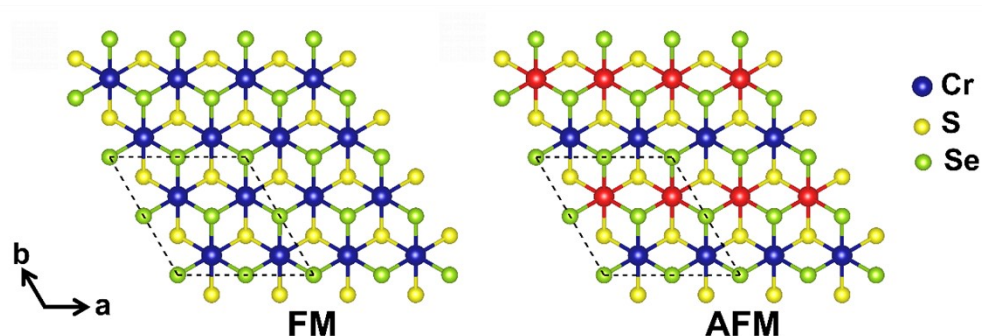


Figure S3 The one FM state and AFM states of $2 \times 2 \times 1$ supercell in CrSSe monolayer. Red and blue respectively represent different spin directions.

5. The spin density of CrSSe monolayer.

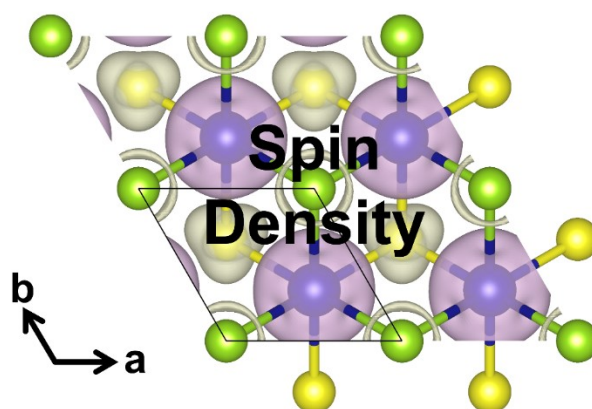


Figure S4 The spin-resolved charge density isosurface (isosurface value = $0.043 e \text{ \AA}^3$) of CrSSe monolayer. Purple and the light-yellow colors represent the net spin-up and spin-down polarization, respectively. Spin polarization is mainly generated by Cr atoms.

6. The SOC-MAE and shape-MAE of free CrSSe monolayer.

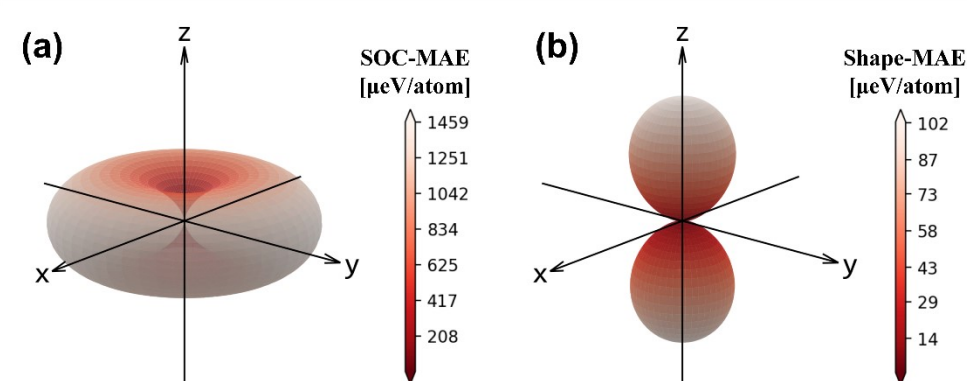


Figure S5 (a) and (b) are schematic diagrams of SOC-MAE and Shape-MAE in the whole space, respectively.

7. Total MAE of CrSSe monolayer under different strains.

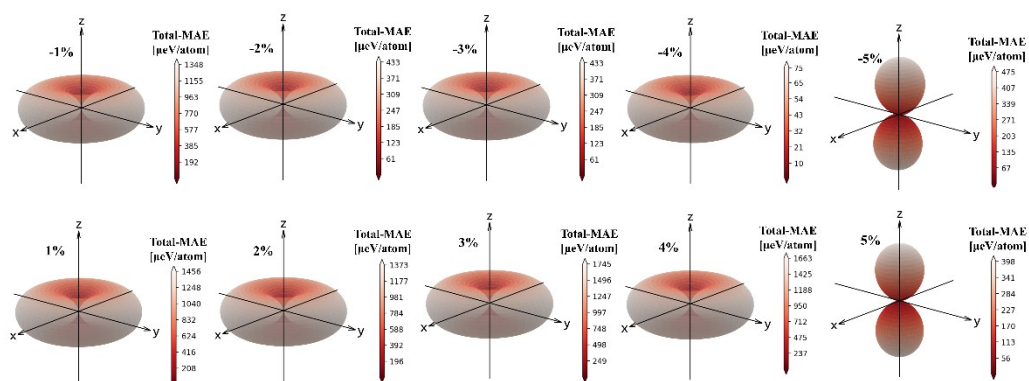


Figure S6 Total MAE of CrSSe monolayer under different strains.

8. The band structures of CrSSe monolayer under different strains.

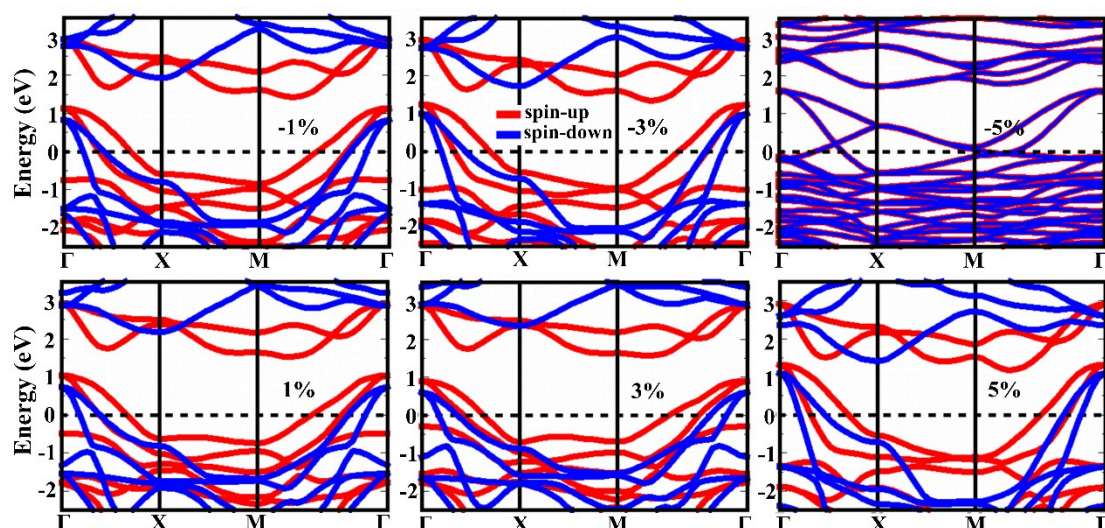


Figure S7 Band structure under biaxial strain. At a compressive biaxial strain of 5%, the CrSSe monolayer is an antiferromagnetic metal.

9. The band structures of CrSSe monolayer under different carrier doping.

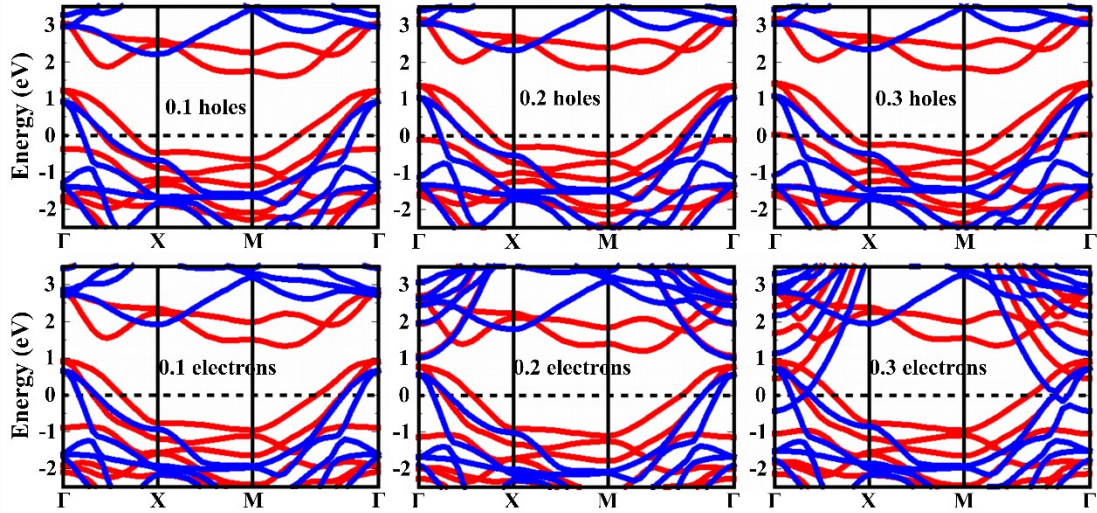


Figure S8 Band structure of doped holes and electrons.

10. Variation of magnetic moments of CrSSe monolayer under external conditions.

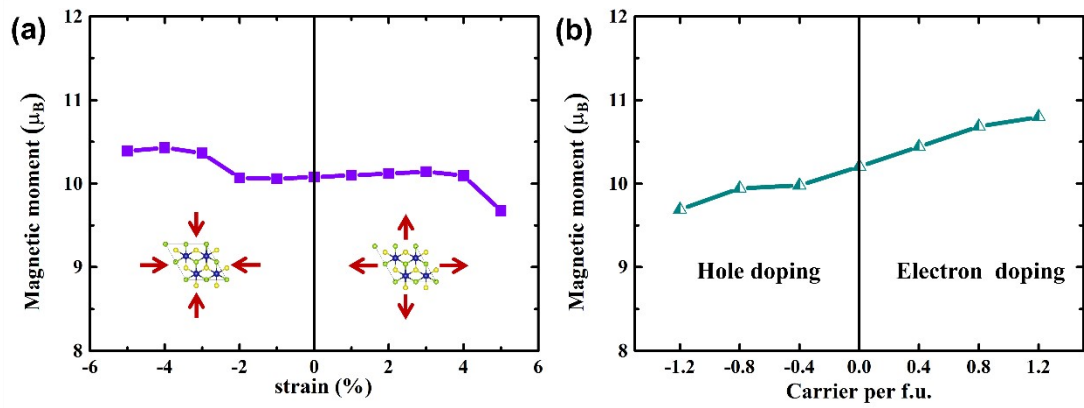


Figure S9 (a) Variation of magnetic moments under different biaxial strains. (b) Changes of magnetic moments under different doping.

11. The Curie temperature of CrSSe monolayer under different strains under external conditions.

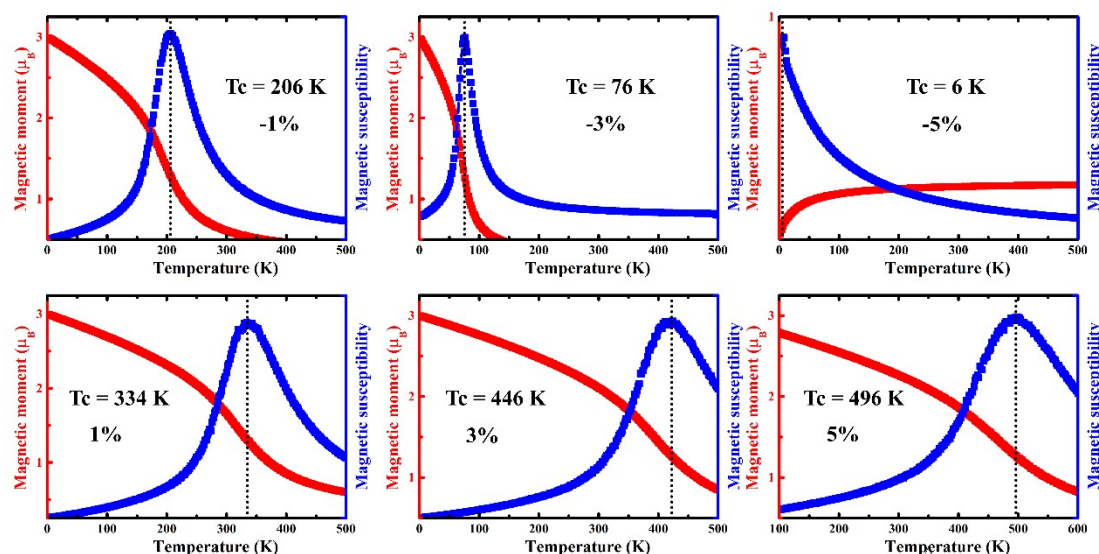


Figure S10 Variation of Curie temperature under different strains.

12. The Curie temperature of CrSSe monolayer under external conditions.

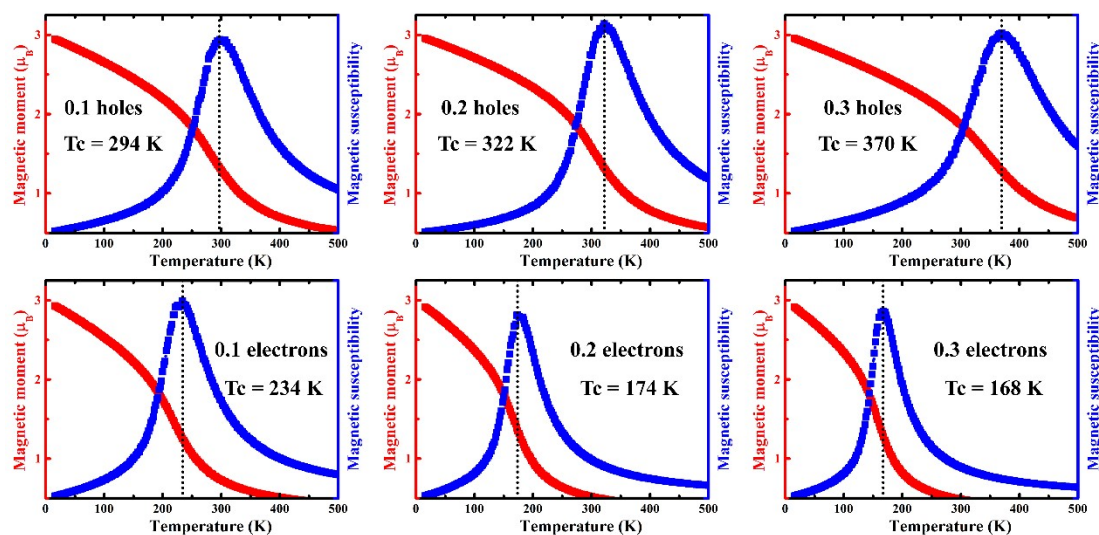


Figure S11 Variation of Curie temperature under different doping.

1. S. M. Alay-e-Abbas, S. Nazir, N. A. Noor, N. Amin and A. Shaukat, *The Journal of Physical Chemistry C*, 2014, **118**, 19625-19634.
2. S. Faiza-Rubab, S. Naseem, E. A. S. M. Alay, M. Zulfiqar, Y. Zhao and S. Nazir, *Phys Chem Chem Phys*, 2021, **23**, 19472-19481.
3. S. Kirklin, J. E. Saal, B. Meredig, A. Thompson, J. W. Doak, M. Aykol, S. Rühl and C.

Wolverton, *npj Computational Materials*, 2015, **1**.

4. S. Peng, W. Kang, M. Wang, K. Cao, X. Zhao, L. Wang, Y. Zhang, Y. Zhang, Y. Zhou, K. L. Wang and W. Zhao, *IEEE Magnetics Letters*, 2017, **8**, 1-5.